Oxidative Cleavage of S–S Bond During the Reduction of Tris(pyridine-2-carboxylato)manganese(III) by Dithionite in Sodium Picolinate–Picolinic Acid Buffer Medium

KALYAN K. SEN GUPTA,[1] NANDINI BHATTACHARJEE,[1] BISWAJIT PAL[2]

[1] *Department of Chemistry, Jadavpur University, Kolkata 700 032, India*

[2] *Department of Chemistry, St. Paul's C. M. College, Kolkata 700 009, India*

Received 29 September 2015; revised 7 June 2016; accepted 16 June 2016

DOI 10.1002/kin.21022

ABSTRACT: The reduction of tris(pyridine-2-carboxylato)manganese(III) by dithionite has been investigated within the temperature window 288–303 K and at pH range 5.22–6.10 in sodium picolinate–picolinic acid buffer medium. The reaction obeys the following stoichiometry:

$$S_2O_4^{2-} + 2Mn^{III} + 2H_2O \rightarrow 2HSO_3^- + 2Mn^{II} + 2H^+$$

The reaction is described in terms of a mechanism that involves an initial complex formation between $S_2O_4^{2-}$ and $[Mn^{III}(C_5H_4NCO_2)_3]$ followed by S–S bond cleavage to give $2HSO_3^-$ and $[Mn^{II}(C_5H_4NCO_2)_2(H_2O)_2]$ as the products via the formation of $SO_2^{\bullet-}$ radical anion. Kinetics and spectrophotometric evidences are cited in favor of the suggested mechanism. Thermodynamic parameters associated with the equilibrium step and the activation parameters with the rate-determining step have been computed. © 2016 Wiley Periodicals, Inc. Int J Chem Kinet 1–9, 2016

INTRODUCTION

Dithionite is a strong reducing agent [1–3] which contains a S–S linkage. The oxidation of thiosulfate that

---

Correspondence to: B. Pal; e-mail: palbiswajit@yahoo.com.

also contains S–S bond has been studied earlier and shown to give tetrathionate by different oxidants such as Ag(III) [4,5], Ir(IV) [6], and Mn(III) [7], and there is no evidence that the S–S bond is cleaved. The thiosulfate ion [8] has the structure of S–SO_3 with a S–S distance of 2.013 ± 0.003 Å. On the other hand, the S–S distance of dithionite is much larger (2.39 Å) than the disulfides and polysulfides, which lies in the region of 2.0–2.15 Å. The long bond is believed to be due to weakening by repulsion of the lone pairs on sulfur atoms that account for its strong reducing property [9]. Considerable amount of work has been done on the oxidation of dithionite by different oxidants. Preliminary research concerning the voltammetric behavior of sodium dithionite indicates that dithionite is oxidized in two steps [10,11]. The kinetics of the oxidation of dithionite by $Fe(CN)_6^{3-}$ and $PtCl_6^{2-}$ have been reported [12,13]. The reduction of manganese(III)-hematoporphyrin [14], toluidine blue [15] in aqueous acidic medium, cytochrome P450 3A4 [16], and neutrophil cytochrome b-558 [17] by dithionite has been studied. Salnikov et al. studied [18] spectroscopically the reduction of cobalamine by dithionite and evidence for the formation of a six-coordinated cobalamine(II) complex has been presented. k_{obs} increases with decreasing pH in the region 13.0–9.0. They have studied the reaction at 298 K. In another publication [19], kinetics and mechanism of cyanocobalamine reduction by sodium hydroxomethane sulfinate (HMS) has been reported. With increasing pH, the reaction rate increases reaching a plateau in the pH range >12.0. The character of the rate-determining step depends on the concentration of the reducing agent when it is in excess. The plot of $1/k_{obs}$ against 1/[HMS] is linear at pH 11.4 and temperature 298 K.

The present report deals with the oxidation of dithionite by tris(pyridine-2-carboxylato)manganese(III) in picolinate–picolinic acid buffer medium with a view to compare the results obtained earlier [7] with sodium thiosulfate and other inorganic reductants by this oxidant.

EXPERIMENTAL

Materials and Methods

The reagents employed were of the highest purity available, and all solutions were made in doubly distilled water. The pH of the Mn(III) solution was recorded to be 5.71. The tris(pyridine-2-carboxylato)manganese(III) complex is unstable either in a high acidic or an alkaline medium. But the complex is reasonably stable within the pH range of 5.14–6.25. The buffer Na(pic)-picH plays a dual role here. One is to maintain the desired pH range, and the major one is to restrict the possibility of ligand substitution reaction that might have occurred between the complex and a buffer other than this one. The ligand substitution reaction is hindered due to the presence of common picolinate ion both in the complex and in the bulk of the reaction medium. Buffer solutions were prepared by mixing calculated amounts of pyridine-2-carboxylic acid ($pK_a = 5.52$) with its sodium salt. The pH of the solution was checked against standard buffer solution with a pH meter (Elico LI 120, Hyderabad, A. P., India). The pH of each buffer solution remained unchanged for a substantial period of time.

Sodium dithionite was purchased from Loba Chemie (Mumbai, India). Sodium dithionite was standardized by the reduction of Fe(III) to Fe(II) using a mixture of thiocyanate and ferrocyanide as an indicator [20]. A deep red coloration of ferric thiocyanate is observed near the end-point of the titration. At the final end-point, the solution rapidly turns blue. Freshly prepared dithionite solutions were always used for the experiments. $Na_2S_2O_4$ solutions are quite stable at pH >5 and in the concentration range (0.2–1.2) × 10^{-3} mol dm^{-3} [21] at which the reactions were studied.

The Mn(III) complex was prepared following the procedures mentioned in the literature [22]. To an aqueous solution of $MnCl_2 \cdot 6H_2O$ (2.5 g in 25 cm^3), H_2O_2 was added. A precipitate of MnO_2 that was formed upon addition of NaOH (1 mg in 25 cm^3) was filtered and washed with water. Excess of pyridine-2-carboxylic acid was added, warmed, and stirred vigorously. The filtrate so formed deposited red crystals of tris(pyridine-2-carboxylato)manganese(III) on cooling. Thermogravimetric analysis indicated a loss of water of crystallization in one step. The compound was then analyzed for C, H, and N. Found C 49.95, H 3.3, N 9.4% calcd for $[Mn^{III}(C_5H_4NCO_2)_3]$ H_2O C 49.92, H 3.2, and N 9.6%. The magnetic moment of the solid compound has been found to be 4.92 BM.

Absorbances were measured on a Systronics (Ahmedabad, Gujrat, India) spectrophotometer. C, H, and N analysis were performed by the Microanalytical Laboratory using a Perkin-Elmer 240C,H,N analyzer (Waltham, Massachusetts, U.S.A.). Thermogravimetric studies were performed on a Shimadzu Corporation's (Tokyo, Japan) TG 50 analyzer in normal atmospheric environment. EPR spectra were recorded with a Varian EPR spectrometer.

The cyclic voltammetric experiment was performed under dry nitrogen using a Bio-Analytical-System (BAS) CV 27 electrochemical analyzer and a BAS model X-Y recorder at 298 K. A standard three electrode electrochemical cell consisting of a platinum disk working electrode (BAS), a platinum wire auxiliary electrode, and a Ag/AgCl reference electrode was used. The cyclic voltammogram of the manganese(III) complex exhibited an irreversible response at 0.8 V, and the corresponding oxidative response was observed at −0.47 V ($\Delta E_p = 330$ mV, $E_{1/2} = -0.63$ V).

The electronic absorption spectrum of the manganese(III) complex exhibits two weak shoulders at approximately 457 and 403 nm ($\varepsilon = 257$ and 407 cm^{-1} mol^{-1} dm^3). Since the extinction coefficients are low in this region, the progress of the reaction was followed spectrophotometrically at 350 nm ($\varepsilon = 2710$ cm^{-1} mol^{-1} dm^3), where the complex absorbs appreciably at the low concentration range of $(1.0–6.0) \times 10^{-4}$ mol dm^{-3}. Moreover, Beer's law is obeyed in this concentration range.

The kinetic studies were carried out under pseudo–first-order conditions, keeping the concentration of dithionite in large excess over that of the manganese(III). Freshly prepared dithionite solutions were always used to ensure reproducibility of the data. Requisite volumes of the reactants at the appropriate temperature were mixed, and the mixture was immediately transferred to a cell of 1 cm path length. The cell compartment of the spectrophotometer was kept at constant temperature. The rate of decrease of manganese(III) was followed for at least two half-lives. Pseudo–first-rate constants (k_{obs}) were calculated from log *A* (where *A* is absorbance) versus time plots. The maximum error in the measurement of rate constant was within 5% depending upon the experimental conditions. However, for most experiments duplicate measurements were reproducible to ±3%.

Stoichiometry and Product Analysis

The stoichiometries of the reactions were studied keeping $[S_2O_4^{2-}]$ in excess over $[Mn^{III}]$ at pH 5.63 and at room temperature (298 K). After completion of the reactions, the excess substrate was determined. The consumption ratio ($\Delta[Mn^{III}]/\Delta[S_2O_4^{2-}]$) was found to be 2.0 (Table I). The observed consumption ratios support the formation of bisulfite as a product of oxidation of $S_2O_4^{2-}$. The formation of bisulfite was confirmed by the tests described below [13].

After the kinetic experiment was over, the reaction product was divided into three parts. Concentrated solution of $Sr(NO_3)_2$ when added to one part of the reaction mixture at pH ∼ 8 gave white precipitate of $SrSO_3$. The solubilization of this white precipitate upon addition of dilute HCl ruled out the formation of sulfate. To the second part of the reaction, the mixture was added zinc acetate, potassium ferrocyanide, and sodium nitroprusside solution. The white precipitate $\{K_2Zn_3[Fe(CN)_6]_2\}$ so formed turned red. When sodium nitroprusside was added to the last part of the reaction mixture in alkali medium, a pink color developed. All these confirmed that bisulfite not the sulfate ion was formed as a reaction product. On the basis of the stoichiometry and product formed, the reactions may be represented stoichiometrically as

$$\begin{aligned} &S_2O_4^{2-} + 2\left[Mn^{III}(C_5H_4NCO_2)_3\right] + 6H_2O \\ &\quad \rightarrow 2HSO_3^- + 2\left[Mn^{II}(C_5H_4NCO_2)_2(H_2O)_2\right] \\ &\quad + 2C_5H_4NCO_2^- + 2H^+ \end{aligned} \tag{1}$$

The liberation of the picolinate ion during the reaction was confirmed [12,23] by the yellow coloration formed on addition of a reagent containing $FeSO_4{\cdot}(NH_4)_2SO_4{\cdot}6H_2O$ (1 g) and KF (0.5 g) in 100 cm^3 of 0.1 N acetic acid to the reaction mixture. The pH of the reaction mixture was checked before and after the reaction, and it was found that the presence of a slight excess of ligand does not alter the pH of the solution. The formation of Mn(II) in the reaction mixture was confirmed by the appearance of typical six lines in the EPR spectrum.

Test for Free Radicals

The polymerization test was carried out by adding 5 cm^3 of 40% (w/v) acrylamide solution to a mixture containing Mn^{III} and dithionite in concentrations 5.0×10^{-4} and 5.0×10^{-3} mol dm^{-3}, respectively, at pH 5.63. The onset of polymerization could not be identified owing to the appearance of turbidity in the initially clear solution. However, when a large excess of methanol was added, a polymeric suspension formed, indicating the intervention of free radicals during the

Table I Stoichiometric Results of the Oxidation of $S_2O_4^{2-}$ by Mn(III)

Initial $[Mn^{III}]$ (10^3 mol dm^{-3})	Initial $[S_2O_4^{2-}]$ (10^3 mol dm^{-3})	Final $[Mn^{III}]$ (10^3 mol dm^{-3})	Final $[S_2O_4^{2-}]$ (10^3 mol dm^{-3})	Δ $[Mn^{III}]$ / $\Delta[S_2O_4^{2-}]$
0.30	1.00	0.00	0.85	1.99
0.40	2.00	0.00	1.81	2.13
0.50	5.00	0.00	4.76	2.08

reaction [24]. Cationic and anionic polymerizations have been ruled out under the conditions at which the reactions were studied. Blank experiments from which either the $S_2O_4^{2-}$ or Mn^{III} was excluded gave no polymeric product.

RESULTS

Effect of $[Mn^{III}(C_5H_4NCO_2)_3]$ and $[S_2O_4^{2-}]$ on k_{obs}

The reactions were studied at various initial concentrations of Mn^{III} in the range (2.0–8.0) × 10^{-5} mol dm^{-3} but at constant $[S_2O_4^{2-}]$, pH, and temperature of 1.0 × 10^{-3} mol dm^{-3}, 5.63, and 288 K, respectively. The average pseudo–first-order rate constant was found to be (20.3 ± 0.5) × 10^{-4} s^{-1}. The reaction is thus first order with respect to $[Mn^{III}]$.

The pseudo–first-order rate constants were also determined (Table II) for different $S_2O_4^{2-}$ concentrations in the range (0.2–1.2) × 10^{-3} mol dm^{-3} but at constant $[Mn^{III}]$ and pH of 4.0 × 10^{-5} mol dm^{-3} and 5.63, respectively. When $1/k_{obs}$ values were plotted against $1/[S_2O_4^{2-}]$, straight lines were obtained making intercepts on the y-axis at different temperatures (Fig. 1), indicating that the reaction between Mn^{III} and $S_2O_4^{2-}$ occurs via an intermediate 1:1 complex formation. Again, the abrupt increase in absorbance at 350 nm on addition of $S_2O_4^{2-}$ to Mn^{III} in a buffer medium is also suggestive of the formation of a complex between the reactants. From the slope and intercept of each plot of $1/k_{obs}$ versus $1/[S_2O_4^{2-}]$, the values of K_e (the equilibrium constant for complex formation) and k_d (the disproportionation constant) were calculated at four different temperatures. The values of K_e and k_d at different temperatures are presented in Table III. The value of K_e was also determined spectrophotometrically at 350 nm using the relation [25–27]:

$$\Delta\varepsilon/C_a = K_e\Delta\varepsilon' l C_0 - K_e\Delta\varepsilon \quad (2)$$

where K_e is the equilibrium constant, l is optical path length in centimeters, C_a is the concentration of the substrate, C_0 is the concentration of manganese(III), and $\Delta\varepsilon$ is difference between the extinction coefficient of the complex and that of manganese(III). From the slope of the plot of $\Delta\varepsilon/C_a$ versus $\Delta\varepsilon$, the spectrophotometric value of K_e was determined to be 4.3 × 10^2 dm^3 mol^{-1} at 288 K.

Table II Effect of Variation of $[S_2O_4^{2-}]$ on the Pseudo–First-Order Rate Constant at Different Temperatures. $[Mn^{III}]$ = 5.0 × 10^{-5} mol dm^{-3} and pH 5.63

10^3 $[S_2O_4^{2-}]$ (mol dm^{-3})	10^3 k_{obs} (s^{-1})			
	288 K	293 K	298 K	303 K
0.4	0.99	1.43	2.08	2.77
0.5	1.20	1.72	2.44	3.45
0.6	1.35	1.96	2.78	4.03
0.8	1.73	2.44	3.57	4.55
1.0	2.03	2.86	4.10	5.41
1.2	2.22	3.23	4.55	6.25

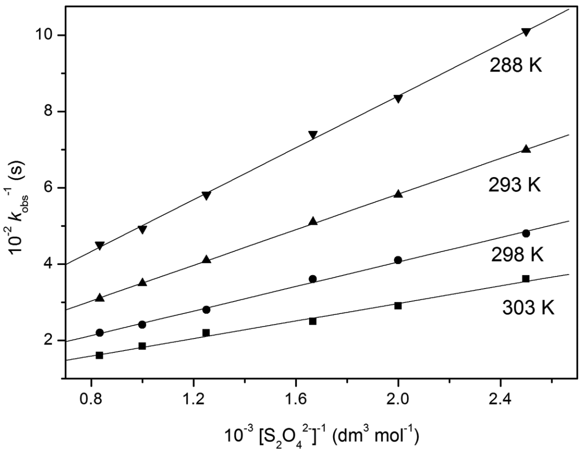

Figure 1 Variation of the reaction rate with $S_2O_4^{2-}$ concentration. Plots of k_{obs}^{-1} versus $[S_2O_4^{2-}]^{-1}$ at four different temperatures. $[Mn^{III}]$ = 5.0 × 10^{-5} mol dm^{-3} and pH 5.63.

Table III Values of Equilibrium Constant for the Fast Step and Disproportionation Constant for the Slow Step at Different Temperatures. $[Mn^{III}]$ = 5.0 × 10^{-5} mol dm^{-3} and pH 5.63

Temperature (K)	K_e (dm^3 mol^{-1})	10^2 k_d (s^{-1})
288	474	0.621
293	502	0.854
298	528	1.18
303	585	1.49

Effect of Variation of Na(pic)-picH

The effect of changing $[H^+]$ (done by varying the concentration ratio of picolinate–picolinic acid) on k_{obs} was also studied in the pH range 5.22–6.10 and at $[Mn^{III}]$, $[S_2O_4^{2-}]$ and temperature of 5.0 × 10^{-5} mol dm^{-3}, 5.0 × 10^{-4} mol dm^{-3}, and 293 K, respectively. Ionic strength was not maintained constant since it has no influence on the reaction rate. The values of k_{obs} were found to be independent at different hydrogen ion concentrations. The absence of the change of rate with change in pH of the buffer system indicates that the concentrations of the ingredients do not have any influence on the reaction.

Activation and Thermodynamic Parameters

The reactions have been studied at different temperatures in the 288–303 K regions. The pseudo–first-order rate constant was found to increase with an increase in temperature (Fig. 1). The thermodynamic parameters (ΔS° and ΔH°) for the equilibrium step and activation parameters ($\Delta H^{\neq}$ and $\Delta S^{\neq}$) for the slowest step in the oxidation of dithionite were calculated from Eqs. (3) and (4) as shown below.

$$\log K_e = [\Delta S^\circ - \Delta H^\circ/T]\, 2.303\ R \tag{3}$$

$$\log (k/T) = [\log (k_B/h) + \Delta S^{\neq}/2.303R] - \Delta H^{\neq}/2.303RT \tag{4}$$

where k_B is the Boltzmann constant, h is Planck's constant, and the other terms have their usual meaning.

DISCUSSION

The rates of decomposition of 5.0×10^{-3} mol dm^{-3} $Na_2S_2O_4$ solution (in terms of the slopes of the concentration–time curves) at 296 K are reported to be 1.85×10^{-6}, 0.7×10^{-6}, 0.28×10^{-6}, and 0.12×10^{-6} mol dm^{-3} s^{-1} at pH values of 3.5, 4.0, 4.5, and 5.0, respectively [10]. At higher pH, the rate of decomposition is even slower. The rate of decomposition of 1.0×10^{-3} mol dm^{-3} $Na_2S_2O_4$ at 296 K and pH 4.5 in the absence of any stabilizing cation was found to be 0.087×10^{-6} mol dm^{-3} s^{-1}. The above results suggest that the hydrolysis of dithionite is too slow to be significant under the studied pH range (5.22–6.10).

Dithionous acid is a strong acid, which ionizes according to Eqs. (5) and (6).

$$H_2S_2O_4 \overset{K_1}{\rightleftharpoons} HS_2O_4^- + H^+ \tag{5}$$

$$H_2S_2O_4^- \overset{K_2}{\rightleftharpoons} S_2O_4^{2-} + H^+ \tag{6}$$

The values of K_1 and K_2 have been reported [3] to be 4.5×10^{-1} and 3.5×10^{-3} at 298 K. Since

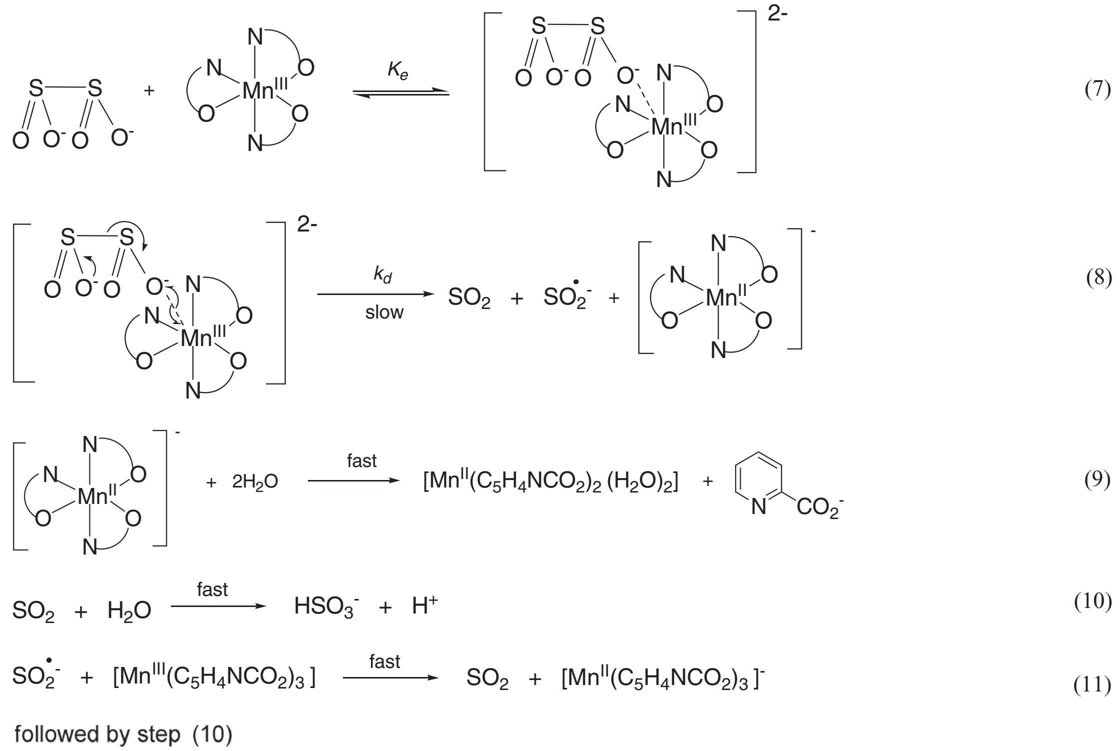

Scheme 1 Overall reaction mechanism involving oxidation of dithionite by Mn^{III}.

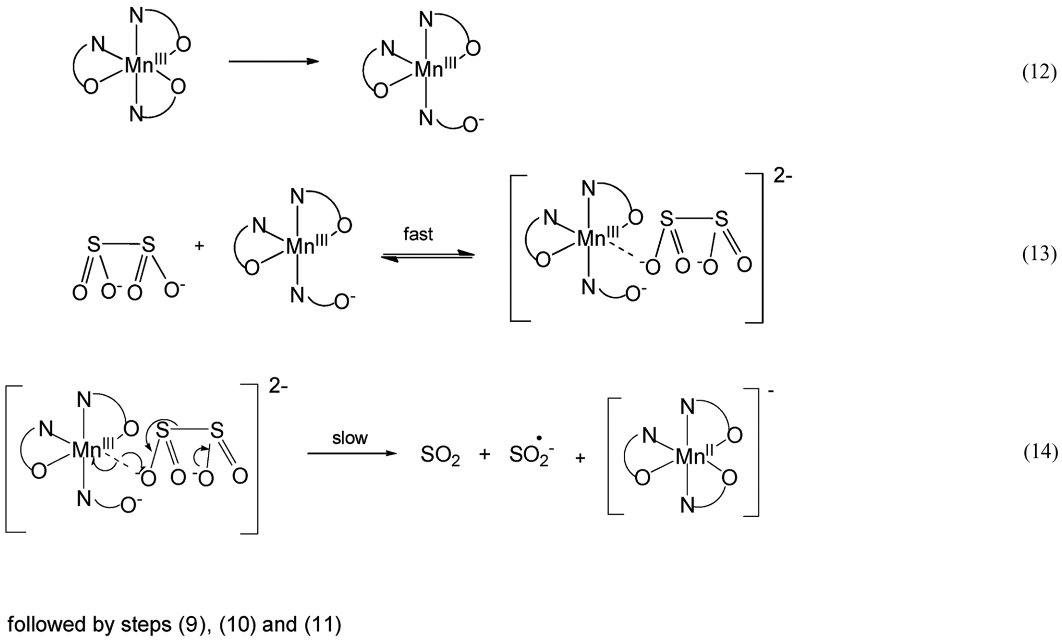

Scheme 2 Alternative reaction mechanism involving oxidation of dithionite by Mn^{III}.

the reaction has been carried out in the pH range 5.22–6.10, it is likely that the $S_2O_4^{2-}$ ion is the predominant reductant species, which reduces Mn^{III}. The oxidation of $S_2O_4^{2-}$ proceeds via a 1:1 intermediate complex formed between $[Mn^{III}(C_5H_4NCO_2)_3]$ and $S_2O_4^{2-}$.

The Mn^{III} complex has been reported to be a distorted octahedron with the axial positions occupied by N atoms [12]. In the intermediate complex, it is quite plausible that the $S_2O_4^{2-}$ moiety occupies the seventh coordination site; the coordination takes place through one of the negatively charged O atoms. The intermediate complex breaks down in the rate-determining step to give SO_2 and the radical anion $SO_2^{\bullet-}$ [11] thereby reducing Mn^{III} to $[Mn^{II}(C_5H_4NCO_2)_3]^-$. The Mn^{II} complex in the presence of water is likely to form the more stable aquated form $[Mn^{II}(C_5H_4NCO_2)_2(H_2O)_2]$ with the liberation of a picolinate ion. The $SO_2^{\bullet-}$ undergoes further one-electron oxidation by another Mn^{III} molecule to give a second molecule of SO_2. Similar observation has also been reported in the kinetic studies of the reduction of $Fe(CN)_6^{3-}$ by the dithionite ion [12] under the stoichiometric ratio of $[Fe^{III}]$:$[S_2O_4^{2-}]$ = 2:1 that suggests the the dissociation of the reductant in the rate-determining step with a subsequent rapid reduction of another $Fe(CN)_6^{3-}$ by the $SO_2^{\bullet-}$ radical ion.

The mechanism suggested for the oxidation of dithionite by $[Mn^{III}(C_5H_4NCO_2)_3]$ is shown in Scheme 1.

An alternative mechanistic pathway (Scheme 2) shows a chelate ring opening in the Mn^{III} complex to give a penta-coordinated species, which binds to the $S_2O_4^{2-}$ moiety. After the electron transfer, the picolinate ion is expected to rechelate. This alternative mechanistic pathway should not affect the rate expression shown below.

The reaction obeys the following rate expression:

$$-\frac{d\left[Mn^{III}\right]}{dt}=\frac{k_d K_e\left[Mn^{III}\right]\left[S_2O_4^{2-}\right]}{1+K_e\left[S_2O_4^{2-}\right]} \tag{15}$$

$$k_{obs}=-\frac{1}{\left[Mn^{III}\right]}\frac{d\left[Mn^{III}\right]}{dt}=\frac{k_d K_e\left[S_2O_4^{2-}\right]}{1+K_e\left[S_2O_4^{2-}\right]} \tag{16}$$

$$\frac{1}{k_{obs}}=\frac{1}{k_d}+\frac{1}{k_d K_e\left[S_2O_4^{2-}\right]} \tag{17}$$

In Scheme 2, the reaction has been shown to take place between two negatively charged ions. The reactions that take place between two similarly charged ions [28,29] are characterized by negative entropies of activation. The present value of $\Delta S^{\neq}$, which is –137 ± 13 J K^{-1} mol^{-1}, supports the suggested step (13) and mechanism. Again oxygen-free dithionite solution shows a strong ESR signal, which indicates that $S_2O_4^{2-}$

dissociates to give $SO_2^{\bullet -}$:

$$S_2O_4^{2-} \rightleftharpoons 2\ SO_2^{\bullet -} \tag{18}$$

The equilibrium was used [30] to study the sulfur dioxide radical ion $SO_2^{\bullet -}$ during the oxidation of dithionite by Co(III), Fe(III), and Mn(III) complexes. Since $[SO_2^{\bullet -}] = K^{1/2}\ [S_2O_4^{2-}]^{1/2}$, the absolute rate constant was calculated using the relation $k = k_{obs}/K^{1/2}[S_2O_4^{2-}]^{1/2}$. On the other hand, during the reduction of electron transfer proteins and other compounds of biological interest by dithionite, the equilibrium constant of $S_2O_4^{2-} \rightleftharpoons 2SO_2^{-}$ has been determined [31] by electron paramagnetic resonance spectroscopy. The equilibrium constant between the monomer form and the dimer form of dithionite has been calculated using different buffers such as sodium pyrophosphate, sodium phosphate, and glycinate in the pH range 7.25–10.4 at constant ionic strength (0.8 M). The values of K have been found to be in the range $(0.85\text{–}1.5) \times 10^{-19}$ M. A reasonable value of the equilibrium constant (K) of the reaction in pyrophosphate buffer at pH 8.0 is $(1.4 \pm 0.4) \times 10^{-9}$ M, which has been utilized in calculating the second-order rate constant for the reaction between the oxidant and SO_2^{-}. The authors [30,31] have calculated rate constants in alkaline medium unlike the present investigation which has been carried out in acid medium.

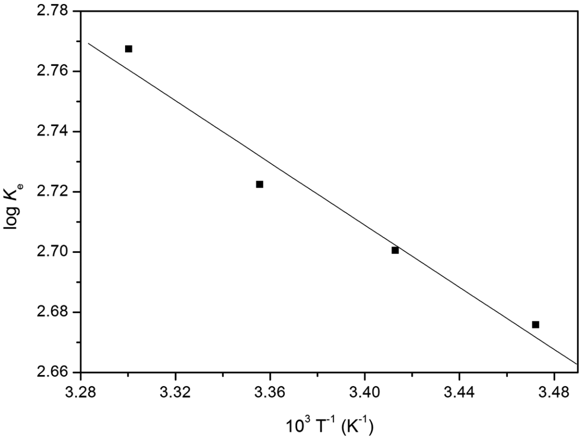

Figure 2 Influence of temperature on the equilibrium constant. Plot of log (K_e/T) versus 1/T. $[Mn^{III}] = 5.0 \times 10^{-5}$ mol dm^{-3} and pH 5.63.

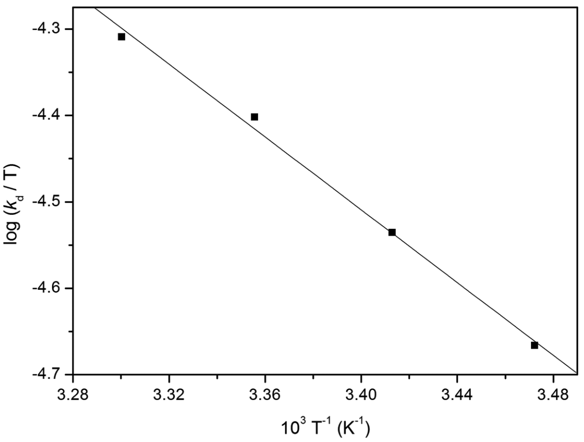

Figure 3 Influence of temperature on the disproportionation constant. Plot of log (k_d/T) versus 1/T. $[Mn^{III}] = 5.0 \times 10^{-5}$ mol dm^{-3} and pH 5.63.

Table IV Experimental and Calculated Pseudo–First-Order Rate Constant Values at 288 K

$10^4\ [S_2O_4^{2-}]$ (mol dm^{-3})	$10^3\ k_{obs\ (expt)}$ (s^{-1})	$10^3\ k_{obs\ (Calcd)}$ (s^{-1})^a
4.0	0.99	0.91
5.0	1.20	1.10
6.0	1.35	1.27
8.0	1.73	1.59
10.0	2.03	1.87
12.0	2.22	2.11

^{a}Calculated k_{obs} values are obtained using the spectrophotometric value of K_e of 430 dm^{-3} mol^{-1} at 288 K.

The plots as shown in Fig. 1 justify the derived rate equation (15). The enthalpy change (ΔH°) associated with the equilibrium step was calculated from the slope of the least-square plot of log K_e versus 1/T (Fig. 2). The corresponding entropy change ΔS° was calculated from Eq. (3). The values of ΔH° and ΔS° are 9.0 ± 2 kJ mol^{-1} and –20 ± 7 J K^{-1} mol^{-1}, respectively. The enthalpy of activation ($\Delta H^{\neq}$) was calculated to be 43 ± 4 kJ mol^{-1} from the slope of the least-squares plot of log(k_d/T) versus 1/T (Fig. 3). The entropy of activation ($\Delta S^{\neq}$) was found to be –137 ± 13 J K^{-1} mol^{-1} using Eq. (4).

The value of K_e obtained from spectrophotometric measurement has been utilized to calculate k_{obs} using the deduced rate expression. The experimental and calculated values are presented in Table IV. It is to be mentioned that freshly prepared solutions of dithionite were used at the beginning of the spectrophotometric experiment to minimize decomposition of dithionite solution. Despite this precaution some decomposition may also occur. However, the observed and calculated values of k_{obs} are not widely different thereby justifying the suggested mechanism and rate expression.

We have earlier investigated the oxidation of some inorganic reducing substrates by this oxidant [32–35]. The values of $\Delta H^{\neq}$ and $\Delta S^{\neq}$ for these reactions have been mentioned in our recent report [7]. The values of

Table V Values of Thermodynamic Parameters for the Oxidation of Different Inorganic Reductants by Mn(III) in Acid Medium

Reductant	Reaction	E^0 (V) [36]	ΔG^0 (kJ mol^{-1})	$\Delta G^{\neq}$ (kJ mol^{-1})
N_3^- [32]	$3N_2 + 2H^+ + 2e \leftrightarrows 2HN_3$	−3.1	598.3	87.8
	$3N_2 + 2e \leftrightarrows 2N_3^-$	−3.4		
NH_2OH [33]	$N_2 + 2H_2O + 4H^+ + 2e \leftrightarrows 2NH_2OH{\cdot}H^+$	−1.87	360.9	37.2
H_3PO_2 [34]	$H_3PO_3 + 2H^+ + 2e \leftrightarrows H_3PO_2 + H_2O$	−0.50	96.5	92.3
H_3PO_3 [34]	$H_3PO_4 + 2H^+ + 2e \leftrightarrows H_3PO_3 + H_2O$	−0.276	53.3	98.3
SO_3^{2-} [35]	$SO_4^{2-} + 4H^+ + 2e \leftrightarrows H_2SO_3 + H_2O$	0.172	−33.2	61.7
$S_2O_3^{2-}$ [7]	$S_4O_6^{2-} + 2e \leftrightarrows 2S_2O_3^{2-}$	0.08	−15.4	72.5
$S_2O_4^{2-}$ (present study)	$2H_2SO_3 + H^+ + 2e \leftrightarrows HS_2O_4^-$	−0.06	10.8	82.5

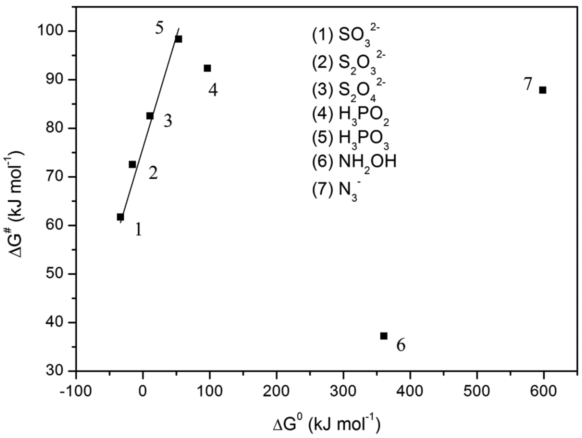

Figure 4 Correlation plot of the thermodynamic parameters in the oxidation of different inorganic compounds by Mn^{III}. Plot of $\Delta G^{\#}$ versus ΔG^0.

$\Delta G^{\neq}$ have been calculated (Table V) using the relation $\Delta G^{\neq} = \Delta H^{\neq} - T\Delta S^{\neq}$ at 288 K. If ΔG^0 is the standard free energy of the elementary electron transfer step in the prevailing electrolyte medium and 2 is the number of electrons transferred, the values of ΔG^0 ($\Delta G^0 = -2FE^0$) have been calculated using the known value [36] of E^0 and are presented in Table V. For weak interaction (neglible overlap between the orbitals in the activated state), Marcus theory predicts [37–39] a slope of ½ for the $\Delta G^{\neq}$versus ΔG^0 plot. This was later on verified by Nikolov [40] for a number of redox reactions. We have also plotted $\Delta G^{\neq}$versus ΔG^0 (Fig. 4). The plot is linear for the reactions when the redox potentials are in the lower region (–0.06 to 0.5 V), whereas for higher E^0 values, e.g., $2N_3^- \rightarrow 3N_2 + 2e$ (–3.4 V) and $NH_2OH \rightarrow N_2 + 2e$ (–1.87 V) the plot is nonlinear (Fig. 4). However, theoretically predicted slope of ½ has been observed from the linear portion of the plot.

Both $S_2O_3^{2-}$ and $S_2O_4^{2-}$, which contain S–S linkage, have been oxidized by different oxidants to give tetrathionate and sulfite, respectively. It has been reported [41] that the ferrate ion ($HFeO_4^-$), which is a powerful two electron oxidant ($E_0 = 1.9$ V) and an oxygen transfer agent, rapidly oxidizes $S_2O_3^{2-}$ to SO_3^{2-} in acid medium when the reductant is in excess to that of oxidant. This is because $S_2O_3^{2-}$ is oxidized initially to give $OSSO_3^{2-}$ and Fe(IV) followed by the reaction of $OSSO_3^{2-}$ with another molecule of the oxidant to give Fe(IV) and $S_2O_5^{2-}$. The latter finally gives SO_3^{2-} by reacting rapidly with water as mentioned below.

$$HFeO_4^- + S_2O_3^{2-} \rightarrow \mathrm{Fe\,(IV)} + OSSO_3^{2-} + H^+ \quad (19)$$

$$HFeO_4^- + OSSO_3^{2-} \rightarrow \mathrm{Fe\,(IV)} + S_2O_5^{2-} + H^+ \quad (20)$$

$$S_2O_5^{2-} + H_2O \rightarrow 2SO_3^{2-} \quad (21)$$

Such a possibility that SO_3^{2-} is formed in the oxidation of $S_2O_3^{2-}$ by manganese(III) has been ruled out since Mn(III) is a less powerful oxidant than $HFeO_4^-$. It is pertinent to compare the oxidation of $S_2O_3^{2-}$ and $S_2O_4^{2-}$ by Mn^{III} as an oxidant. There are few similarities in these two reactions. Both the reactions occur through intermediate formation of free radicals and also through the inner sphere reduction process. The formation of Mn^{II} in both these reactions has been confirmed by the appearance of typical six-line EPR spectrum. On the other hand, there is no evidence that the S–S bond is broken in the oxidation of thiosulfate where the substrate is oxidized to give tetrathionate and no complex formation occurs prior to electron transfer unlike the oxidation of dithionite where the reaction occurs through intermediate formation of complex between the two reactants followed by the decomposition to give products. The activation parameters obtained in the oxidation of dithionite are different from thiosulfate oxidation there by supporting different mechanism and S–S bond cleavage.

CONCLUSION

The redox reaction between dithionite and Mn^{III} in picolinate–picolinic acid buffer proceeds through the formation of 1:1 intermediate complex. The reaction involves a one-electron transfer process from $S_2O_4^{2-}$ to Mn^{III} with subsequent cleavage of the S–S bond in the slow step, which ultimately ended to form HSO_3^-.

BIBLIOGRAPHY

1. Cotton, F. A.; Wilkinson, G. Advanced Inorganic Chemistry, 3rd ed., Wiley Eastern: New Delhi, India, 1979; p. 451.
2. Mellor, J. W. A Comprehensive Treatise on Inorganic and Theoretical Chemistry, vol 10; Longman: London; 1904; pp. 288, 375.
3. Page, F. M. Trans Faraday Soc 1953, 49, 635–643.
4. Rush, J. D.; Kirschenbaum, L. J. Inorg Chem 1985, 24, 744–748.
5. Kirschenbaum, L. J.; Panda, R. K.; Borish, E. T.; Mentasti, E. Inorg Chem 1989, 28, 2623–2630.
6. Sen Gupta, K. K.; Das, S.; Sen Gupta, S. Transition Met Chem 1988, 13, 155–159.
7. Sen Gupta, K. K.; Bhattacharjee, N.; Pal, B. Asian J Chem 2015, 27, 2669–2674.
8. Baggio, S. Acta Cryst 1969, 25, 5119.
9. Cotton, F. A.; Wilkinson, G. Advanced Inorganic Chemistry, 3rd ed.; Wiley Eastern: New Delhi, India, 1979, p. 452.
10. Govaert, F.; Temmerman, E.; Westbroek, P. Anal Commun 1998, 35, 153–156.
11. Govaert, F.; Temmerman, E.; Kiekens, P. Anal Chim Acta 1999, 385, 307–314.
12. Scaife, C. W. J.; Wilkins, R. G. Inorg Chem 1980, 19, 3244–3247.
13. Pal, B.; Sen Gupta, K. K. Transition Met Chem 2012, 37, 671–678.
14. James, J.; Hambright, P. J Coord Chem 1973, 3, 183–186.
15. Hamza, S. A.; Iyun, J. F.; Irdis, S. O. J Chem Pharm Res 2012, 4, 6–13.
16. Davydov, D. R.; Fernando, H.; Baas, B. J.; Sligar, S. G.; Halpert, J. R. Biochemistry 2005, 44, 13902–13913.
17. Aviram, I.; Sharabani, M. Biochem J 1986, 237, 567–572.
18. Salnikov, D. S.; Dumitrescv, R. S.; Makarov, S. V.; Van Eldik, R.; Boss, G. R. Dalton Trans 2011, 40, 9831–9834.
19. Salnikov, D. S.; Derevenkov, I. A.; Artyushina, E. N.; Makarov, S. V. Russ J Phys Chem 2013, 87, 44–48.
20. Hahn, F. L. Anal Chim Acta 1949, 3, 62–64.
21. Lem, W. J.; Wayman, M. Can J Chem 1970, 48, 776–781.
22. Ghosh, S.; Ray, R. K.; Bandopadhyay, T. K.; Deb, A. K. Z Naturarch 1981, 36B, 1270.
23. Sen Gupta, K. K.; Bhattacharjee, N.; Pal, B.; Ghosh, S. Transition Met Chem 1999, 24, 268–273.
24. Sen Gupta, K. K.; Pal, B.; Begum, B. A. Carbohydr Res 2001, 330, 115–123.
25. Klaning, U. Acta Chem Scand 1957, 1, 1313–1316.
26. Sen Gupta, K. K.; Dey, S.; Sen Gupta, S.; Adhikari, M.; Banerjee, A. Tetrahedron 1990, 46, 2431–2444.
27. Sen Gupta, K. K.; Bhattacharjee, N. Int J Chem Kinet 2002, 34, 411–417.
28. Frost, A. A.; Pearson, R. G. Kinetics and mechanism (2nd ed.); Wiley Eastern: New Delhi, India, 1970, p. 144.
29. Panchenkov, G. M.; Lebedev, V. P. Chemical Kinetics and Catalysis; Mir: Moscow, 1976; p. 238.
30. Neta, P.; Huie, R. E.; Ross, A. B. J Phys Chem Ref Data 1988, 17, 1027–1284.
31. Lambeth, D. O.; Palmer, G. J Biol Chem 1973, 248, 6095–6103.
32. Sen Gupta, K. K.; Pal, B.; Bhattacharjee, N.; Ghosh, S. P. Bull Chem Soc Jpn 1999, 72, 1769–1774.
33. Sen Gupta, K. K.; Pal, B. Inorg React Mech 2000, 1, 265–272.
34. Sen Gupta, K. K.; Bhattacharjee, N. Transition Met Chem 2000, 25, 518–521.
35. Sen Gupta, K. K.; Bhattacharjee, N. J Indian Chem Soc 2001, 78, 284–286.
36. Lurie, J. Handbook of Analytical Chemistry; Mir: Moscow, 1975; pp. 307, 309, 311.
37. Marcus, R. A. J Chem Phys 1956, 24, 966–978.
38. Marcus, R. A. J Phys Chem 1963, 67, 853–857.
39. Marcus, R. A. Pure Appl Chem 1997, 69, 13–29.
40. St. Nikolov, G. Inorg Chim Acta 1971, 5, 559–562.
41. Johnson, M. D.; Read, J. F. Inorg Chem 1996, 35, 6795–6799.